Experimental and analytical flexural performances of reinforced concrete beams strengthened with post-tensioned near surface mounted basalt composite laminates

Lluís Gil, Ernest Bernat & Christian Escrig

Department of Strength of Materials and Structures in Engineering
Technical University of Catalonia UPC
ESEIAAT, c/ Colom 11, 08222, Terrassa, Spain

Keywords: strengthened RC beams, NSM, BFRP, post-tensioning

Abstract

Near surface mounted (NSM) is a technique that improves the strengthening capacity of composite laminates. The use of a post-tensioning technique modifies the performance of the strengthening because it is active bearing loads from the very beginning. This study compares the performances of three beams: one without strengthening, one with passive NSM laminate, and a third with post-tensioned NSM laminate. The experimental approach compares the pre-cracking and post-cracking performance until failures, showing that the post-tensioned solution withstands larger loads in pre-cracking and presents less deformation in post-cracking. Moreover, post-tensioning is an effective technique that can prevent loss of stiffness even after cracking. Finally, simple analytical equations based on the plane cross-section for pre-cracking and failure analysis are proposed, showing good agreement with the experimental results.

1. Introduction

Fibre reinforced polymer (FRP) materials provide solutions for strengthening reinforced concrete (RC) beams. Pioneering solutions bonded FRP laminates on the surface of beams for shear and bending strengthening. Transmission of stresses from the substrate to the composite occurs through the contact surface. Therefore, it is expected that a larger bonded surface will provide a more efficient and safer solution. Thus, near surface mounted (NSM) solutions have become a competitive alternative because they provide a clear increase in the contact surface. The technique is briefly described in FIB Bulletin 14 [1].

Pioneering studies on introducing an initial stress state to FRP members were performed by Nordin and Taljsten [2], who tested several RC beams prestressed with NSM carbon fibre reinforced polymer (CFRP) strips. The results showed that this technique could increase the first-crack and stress-yielding loads. Subsequently, Badawi and Soudki [3] also prestressed NSM CFRP rods in four beams and achieved an increase in the ultimate load of 79%. Peng et al. [4] developed a comprehensive experimental programme for NSM-strengthened RC beams including prestressed members. The effect of various parameters on the behaviour and failure of beams were compared, such as the bond length, prestressing force, and anchorage. Results showed that prestressed NSM FRP strips improved the load-carrying capacity of flexural members by up to 122% compared to a non-strengthened beam and by 44% compared to non-prestressed FRP strips. Kara et al. [5] developed a numerical method for estimation of the curvature, deflection, and moment capacity of RC beams strengthened with prestressed NSM FRP strips, and validated the method with experimental results from the literature. Hong et al.

[6] tested eight beams strengthened with NSM CFRP prestressed plates and detected a failure mode in the concrete cover separations at one end of the plates. The technique increased the cracking capacity, yield, and ultimate loads of the beams. Hosseini et al. [7] applied prestressed NSM CFRP to RC slabs; subsequently, Hosseini et al. [8] strengthened slabs of low-strength concrete using NSM CFRP laminates with different prestressing levels.Moreover, Kotynia et al. [9] developed an experimental programme consisting of three series of RC slabs with varying longitudinal steel reinforcement ratio, concrete strength, strengthening adhesion, and preloading level. The results showed improvement in the ultimate and serviceability limit states. Si-Larbi et al. [10] described a strengthening technique involving preloading the FRP rod before mortar casting. Experimental results and numerical analysis were then compared with other externally bonded CFRP and NSM analyses performed by other authors. Rezazadeh et al. [11] proposed a simplified analytical formulation to predict the flexural performance of RC beams strengthened with prestressed CFRP for externally bonded reinforcement (EBR) and NSM techniques. The precracking, postcracking, and postyielding stages define three linear moment–curvature relationships that characterise the flexural behaviour of CFRP strengthened beams. El-Hacha et al. [12] performed an experimental investigation of the effectiveness of using prestressed NSM CFRP bars to strengthen RC beams. Enhancement of the cracking, yielding, and ultimate values were investigated for varying prestressing levels of the embedded NSM CFRP. Kotynia and Przygocka [13] studied the efficiency of prestressing strips in RC beams. Aslam et al. [14] performed a comprehensive literature review of RC post-tensioned NSF FRP strengthening solutions and the flexural performance of these beams. The techniques considered included NSM, EBR, and externally post-tensioned (EPT) techniques. The post-tensioned materials included aramid fibre reinforced polymers (AFRP), carbon fibre reinforced polymers (CFRP) and glass fibre reinforced polymers (GFRP) in the form of rods, strips, plates, and laminates. From the comparison, the authors concluded that the NSM technique provides a safer protection of the post-tensioned strengthening material against the environment, and it may improve the cracking, yielding, and ultimate loads more effectively than other techniques. Michels et al. [15] presented an updated and complete discussion of state-of-the-art prestressed FRP systems. Finally, Zhang et al. [16] focused a state-of-the-art review on the flexural strengthening of RC beams with NSM CFRP strips. They also performed an intensive study on interface bond behaviour and debonding failures.

Anchoring is one of the most critical issues during prestressing. One approach is to use end-anchorage devices like those proposed by Pellegrino and Modena [17]. Recently, Michels et al. [18] proposed an anchorage transfer through the 'gradient method'. This new method is based on the ability of epoxy resin to cure rapidly at high temperatures. Therefore, it is possible to apply heat locally and produce a gradual decrease in the initial prestress force toward the ends of the strip.

Strengthening techniques are normally aimed at recovering the capacities of corroded RC structures. Triantafyllou et al. [19] discovered the difficulties that arise when engineers develop calculation models for assessing steel bar mass loss. They used available experimental results and analytical approaches to propose a model, which was validated against 51 non-strengthened corroded beams and 24 corroded beams strengthened with FRP. Moreover, Triantafyllou et al. [20] and [21] also attempted to strengthen RC beams with different levels of steel corrosion and mass loss. They applied a solution of cement-based repair patch and EBR or NSM FRP laminates. Finally, FRP strengthening may also affect other failures like fatigue, as reported in experimental [22] and analytical [23] studies by Charalambidi et al. It is also worth

mentioning that future works might include the concomitant effects of prestressed FRP strengthening performance with corrosion levels and/or a fatigue comparison.

The present study introduces a new composite made of basalt fibre, which has not yet been tested with any prestressing technique. An experimental programme compares the performance of an RC beam, a NSM basalt fibre reinforced polymer (BFRP) with no prestressing, and a NSM BFRP with prestress introduced by tensing the laminate within the concrete slits. Owing to the construction process, we would rather focus on post-tensioning instead of prestressing techniques. Finally, a sectional analysis is used to develop an analytical formulation aimed at determining the cracking moment and ultimate moment of the tested beams.

2. Materials and methods

2.1 Programme outline

Three RC beam specimens were manufactured and tested: the first was a RC control beam without strengthening, the second was a control beam strengthened with a NSM laminates of composite BFRP which were not post-tensioned, and the third was strengthened with post-tensioned NSM BFRP laminates.

Figure 1 shows the cross-section geometries and reinforcement details of the specimens. The beam cross-sections were (b) 200 mm x (h) 400 mm with a length of 4500 mm. All beams were reinforced with 12 mm steel bars: two were placed on the top and two on the bottom of the beam, with adistance (d) of 25 mm to the beam edges. For shear reinforcement, 8 mm stirrups were spaced at 200 mm. The edges of the stirrups were fastened to the bottom rebars to develop sufficient shear strength. All beams had several slits with dimensions of 50 mm x 5 mm prepared along the beam for embedding the FRP laminates with dimensions of 50 mm x 2 mm using resin (Figure 2).

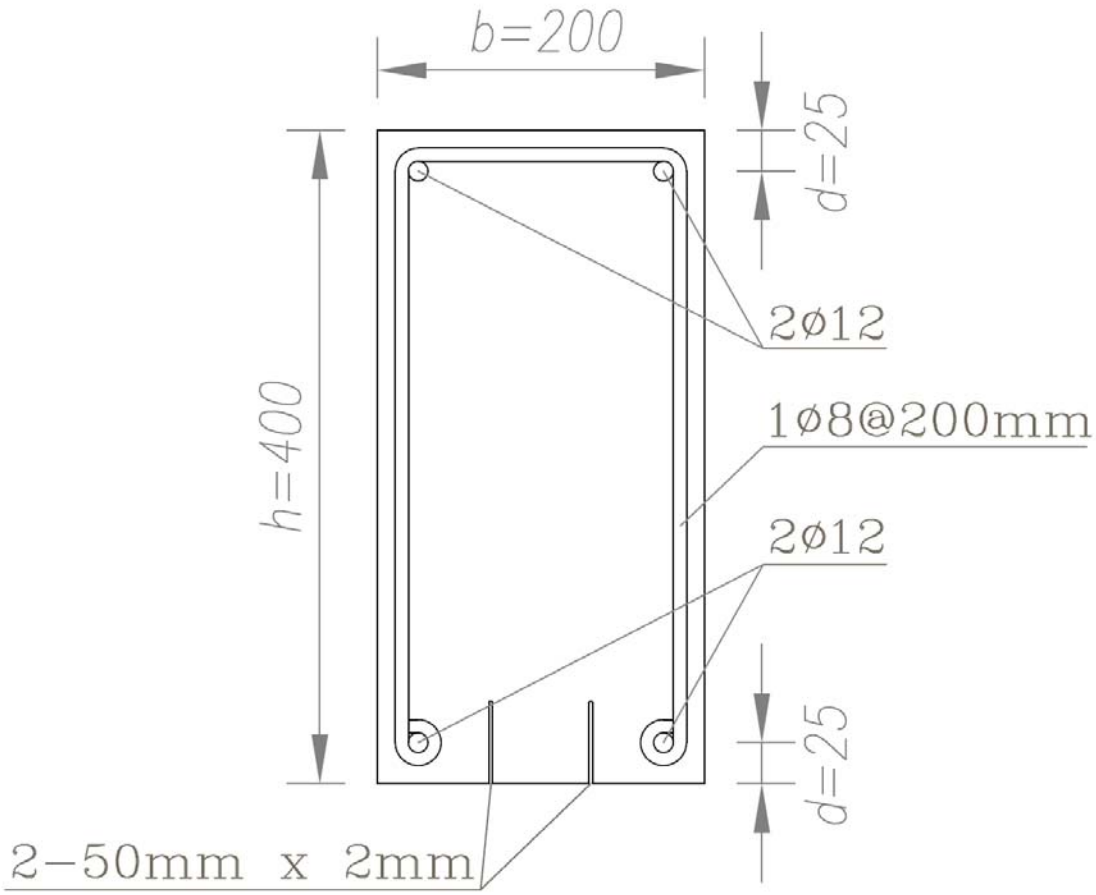

Figure 1. Beam geometry and reinforcement cross-section

Figure 2. Detail of slits for embedding FRP laminate

2.2 Materials and specimens

All material properties used for the analytical calculations are summarised in Table 1.

2.2.1 Concrete and steel

All beams were cast from a single batch of concrete supplied by a local concrete company. The average 28-day compressive strength of the concrete was 30 MPa according to the procedures in EN 12390 [24]. The steel was B-500-S;; no coupons were tested.

2.2.2 BFRP laminates

Composite laminates were manufactured under laboratory conditions using unidirectional basalt fabrics. The basalt fabric properties were provided by the supplier, which reported an ultimate tensile strength 3080 MPa, Young's modulus 95 GPa, and ultimate tensile strain of 3.15%.% The resin used was a bi-component epoxy and polyamide with an ultimate tensile strength of 12 MPa, Young's modulus of greater than 700 MPa, and rupture strain of 40% according to documentation provided by the producer.

Four laminates were manufactured using the hand lay-up method, each with 4 layers of basalt fabric (Figure 3) and resin (Figure 4). The resulting composition of the laminate was 70% fibre and 30% resin by weight. The laminate cross section had dimensions of 50 mm x 2 mm and a length of 5000 mm. The thickness of laminate was measured with a calliper. Four 250-mm-long coupons were cut from two of the laminates and subjected to a tensile test according to the procedure in EN ISO 527-4 [25]. The mean value of the laminate ultimate strength was 450 MPa with a standard deviation of 2.4 MPa. A strain gage was attached to one of the coupons and the Young's modulus was estimated as 22 GPa during a tensile test under elastic conditions according to the procedure proposed by Lord and Morell [26].

The same resin was later poured into the slits to bond the NSM composite laminate to the concrete.

Table 1. Material properties

Material	Tensile strength (MPa)	Compressive strength (MPa)	Young's modulus (GPa)
Concrete		$f_c = 30$	
Steel (values from supplier)	$f_{ys} = 500$		$E_s = 210$
BFRP laminate	$f_{frp} = 450$		$E_{frp} = 22$

Figure 3. Basalt fabric strips

Figure 4. Hand lay-up manufacturing of basalt composite FRP

The maximum strain of the composite laminate can be calculated from the data in Table 1 as follows:

$$\varepsilon_{u,frp} = \frac{f_{frp}}{E_{frp}} = 20‰ \quad (1)$$

Where $\varepsilon_{u,frp}$ is the ultimate strain value for the FRP laminate, f_{frp} is the ultimate stress of the FRP laminate, and E_{frp} is the Young's modulus of the FRP laminate.

2.3 Manufacture of specimens

All beams were cast in a single operation. Slits were crafted for later insertion of the laminates. Slits were prepared in the mould; however, owing to their small size, they showed small geometric flaws. These flaws were mechanically removed from the BFRP NSM beams using an angle grinder. Grooving is a construction issue that should be considered by future practitioners if the flaws are ever large enough to complicate the positioning of laminates. Therefore, practitioners should use water at high pressures or grinders to improve the geometry of slits before inserting the laminates.

The three specimens included one control beam with no additional strengthening as a pristine control sample, labelled RC-control. The second specimen was a control beam strengthened with NSM composite laminate without post-tensioning, labelled FRP-control. Finally, the third

specimen was a beam strengthened with NSM post-tensioned composite laminates, labelled FRP-post-tensioned.

2.3.1 Strengthening of the FRP-control specimen

The beam was positioned upside down with the slits on the upper side. Laminates were instrumented with strain gages on the half span cross-section (Figure 5). The laminates were then introduced to the slits and resin was poured in until all of the slits were filled. The process was completed in less than 15 min, and the curing process was started at room temperature. A slight increase in the temperature in the slits indicated that the resin had begun curing. Complete hardening of the resin took 48 h, after which the beam was ready for testing.

Figure 5. Strain gage installation on the BFRP laminate

2.3.2 Strengthening of the FRP-post-tensioned specimen

The beam was again positioned upside down with the slits on the upper side, as for the FRP-control (Figure 6). The laminates were instrumented with strain gages on the half span cross-section. The laminates were then introduced to the slits and were gripped to a pulling system at one end, while the grip was fixed at the other end (Figure 7). The laminates were pulled to a load of 25 kN, as measured by the load cell on the pulling system (Figure 8). Both laminates were pulled simultaneously, and strain gage measurements confirmed that both laminates performed equally (Figure 9). The grips were then temporarily clamped with auxiliary steel tools and the pulling system was released, transferring all of the force from the actuator to the clamped grips at both ends of the beams. Thus, the load decreases to zero at the end of Figure 10, while the strain gages maintain the strain achieved in Figure 9. This operation took less than 2 min to complete.

Figure 6. Positioning of laminates inside slits

Figure 7. Grips for clamping and pulling of the laminates

Figure 8. Pulling system with actuator

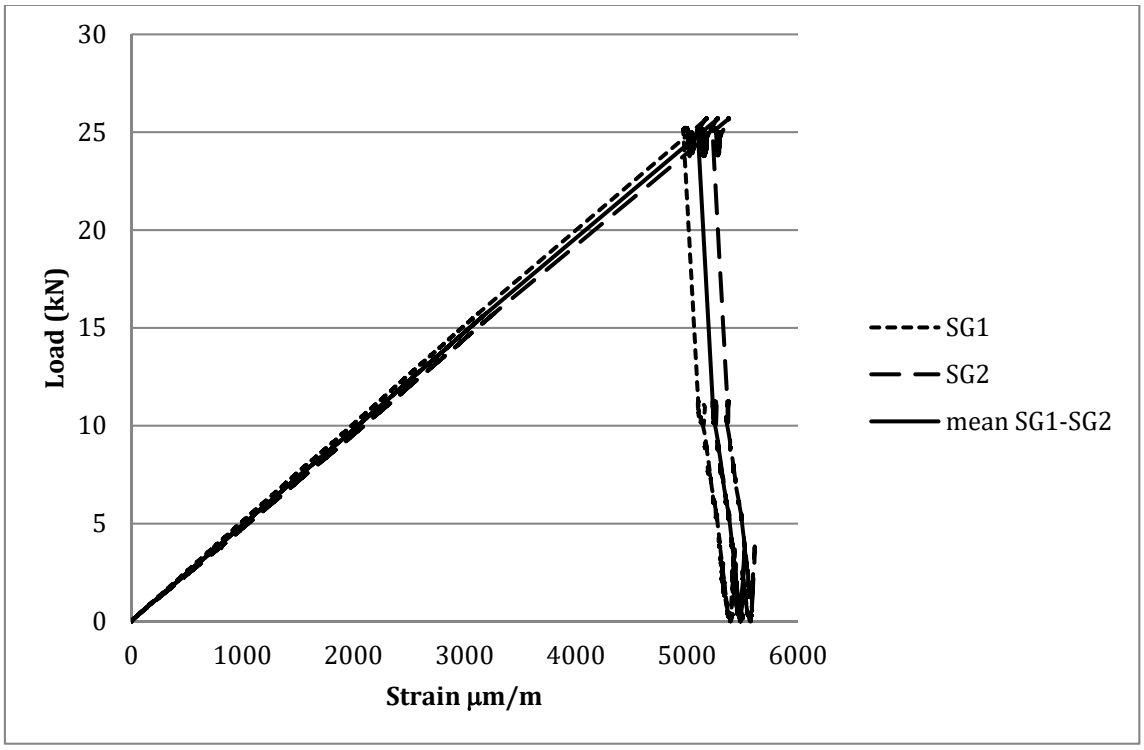

Figure 9. Strain gage measurements during the pulling and clamping operations

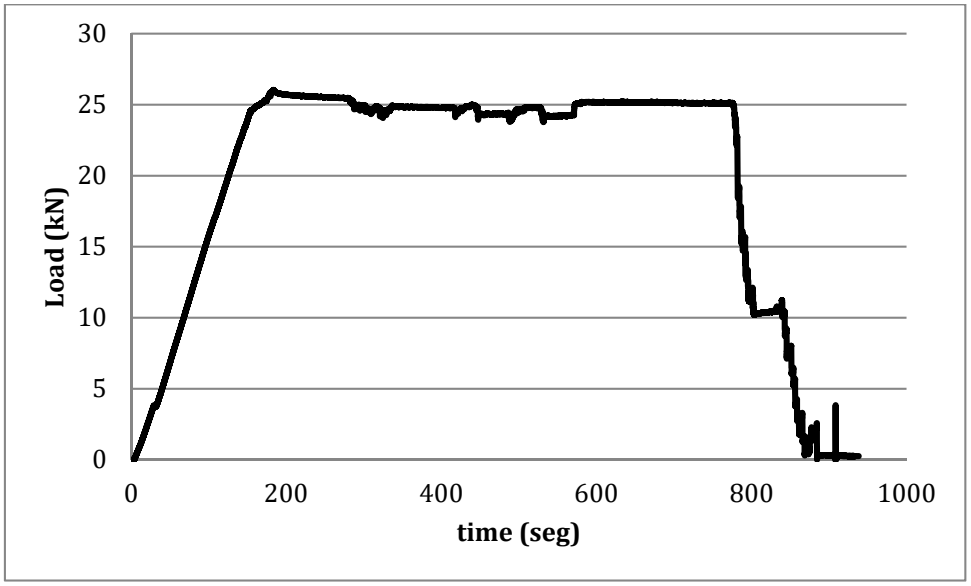

Figure 10. Load history of the pulling system, including pulling to 25 kN (0–200 s), clamping the edges (200–800 s), and releasing the system (800–900 s)

After the laminates were post-tensioned and stabilised, resin was poured into the slits. The operation took 15 min, similar to that of the non-post-tensioned beam. The laminates were continuously monitored with the strain gages until testing. Losses of tension were important during the first 10 h of the curing process. After 48 h, the clamped grids were released and

monitoring continued for an additional 48 h. No additional relevant changes were observed during this last period. The whole tensions loss process is shown in Figure 11.

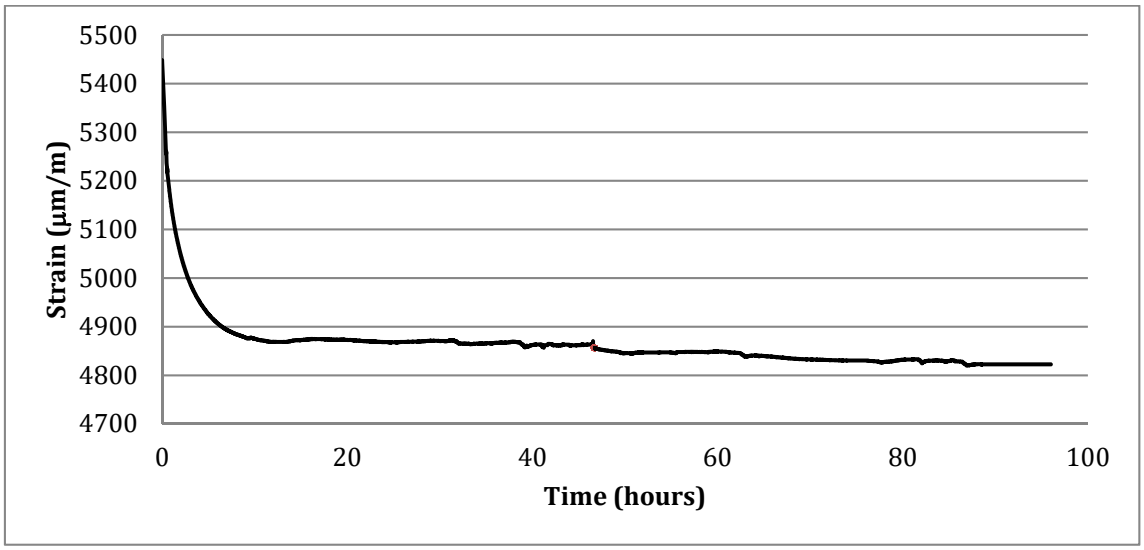

Figure 11. Tension losses in laminates during the curing process (48 h), releasing of the grips (several minutes), and stabilisation (48 h) before beam testing

3. Results

All beams were tested using a standard three point bending test setup. The free span was 4 m between simple supports. A load was first applied in a loading and unloading cycle under displacement control with a displacement rate of 1 mm/min. The first load was applied until cracking of the specimens, and was then unloaded. Curves for the three specimens are shown in Figure 12. Cracking was detected by simple inspection and a small drop in the loading branch.

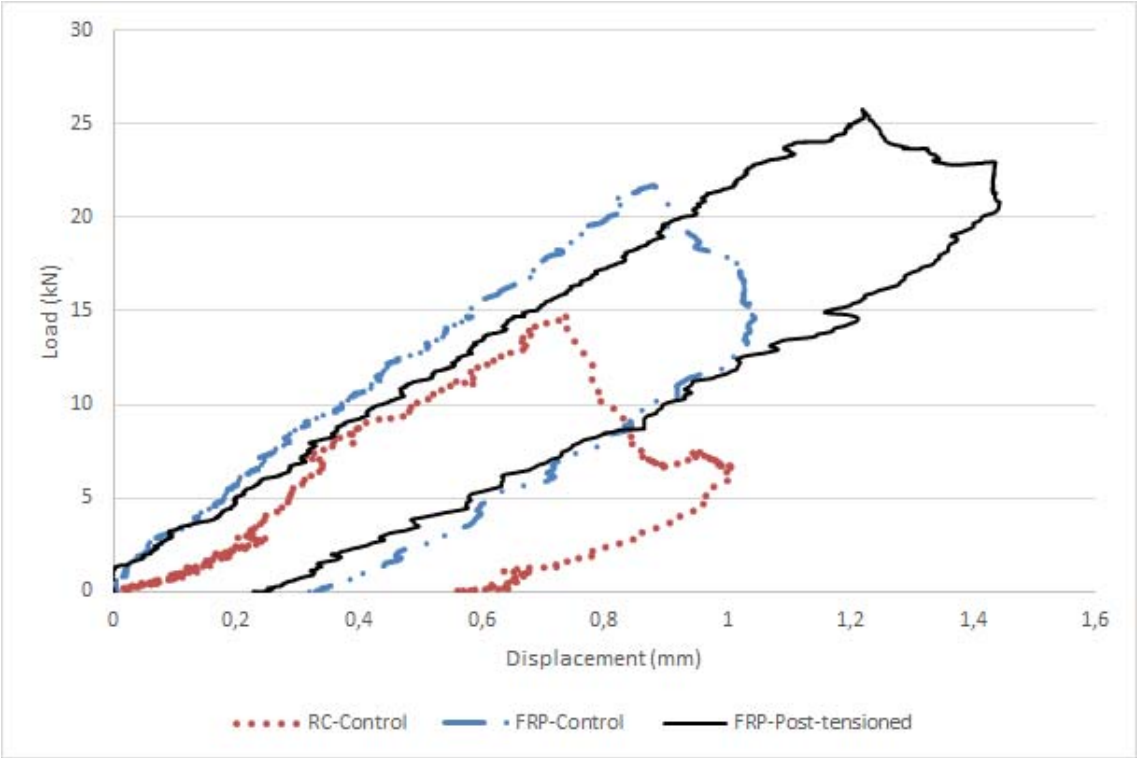

Figure 12. First loading-unloading cycle until for each specimen until the cracking moment

The strain gages on the FRP composite laminates installed in the centre of beam recorded the strain (Figure 13) during the first loading cycle. It should be noted that Figure 13 shows the strain increments with a zero offset at the beginning of the tests. Nevertheless, it is important to remember that the post-tensioned beam began the tests with a pre-strained state of 4820 μm/m. The beams were unloaded once the cracking moment was reached.

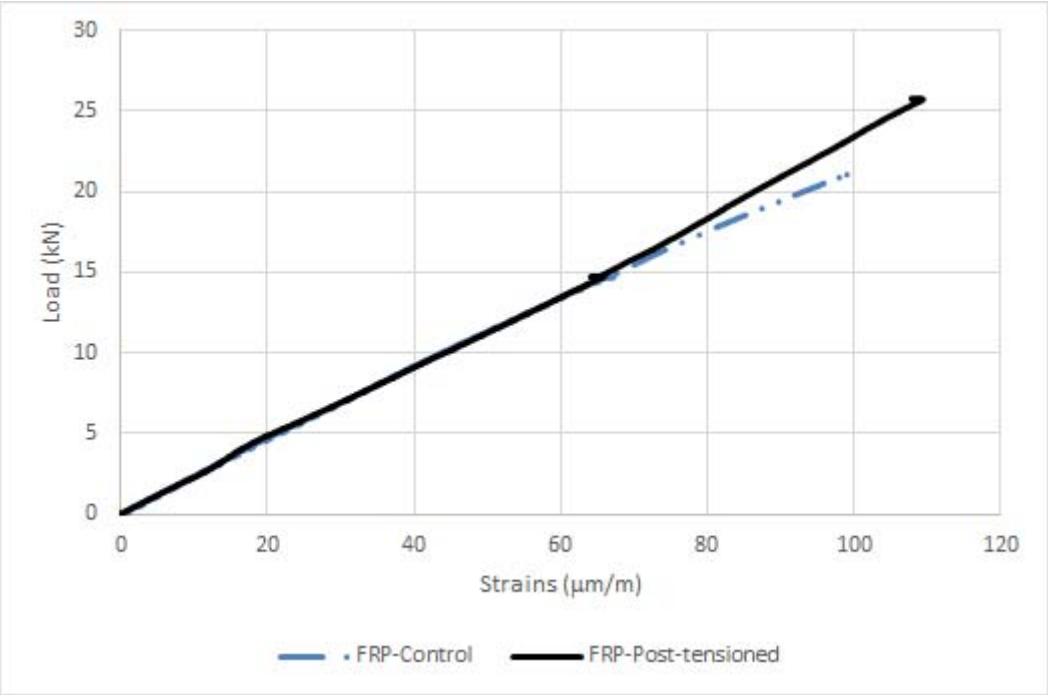

Figure 13. Strain gage measurements in the centre of the beam during the first load cycle for specimens with FRP reinforcement

A second load cycle was then begun and continued with a displacement control rate of 5 mm/min until failure of the beams occurred. Figure 14 shows the load–displacement curves for the specimens, while the strain gage measurements are shown in Figure 15. Here, the strain includes the stress state of the FRP laminate for the post-tensioned beam.

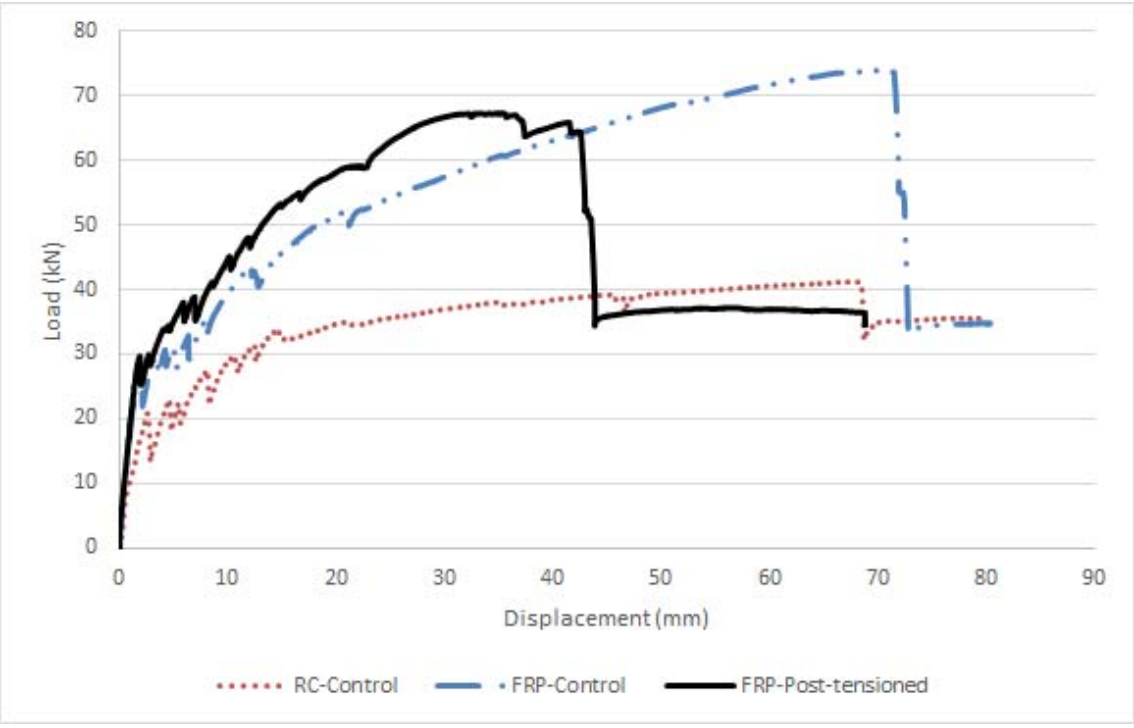

Figure 14. Load–displacement curves for the second load cycle until failure

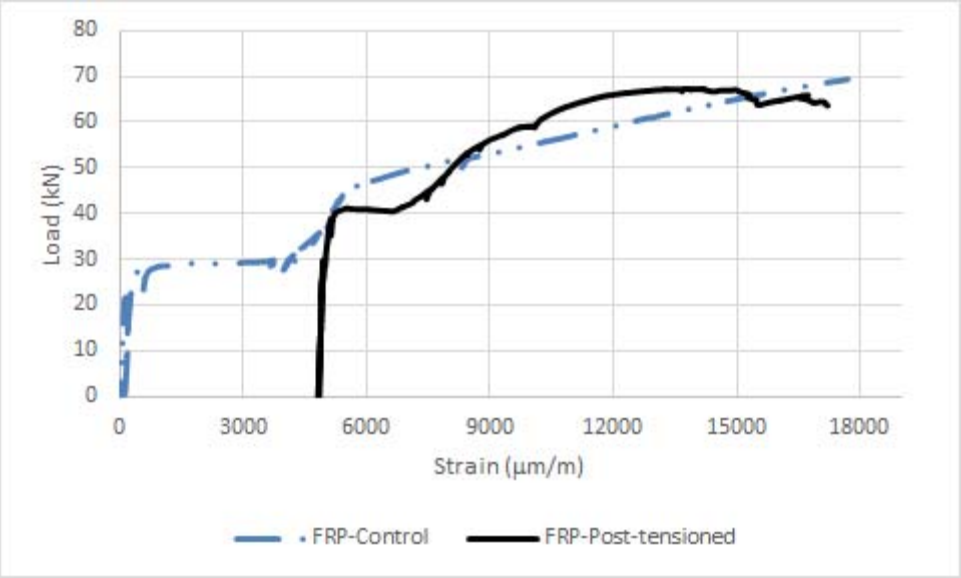

Figure 15. Strain gage measurements in the centre of the beam during the second load cycle for specimens with FRP reinforcement

Figure 16. Failure of the RC-control beam

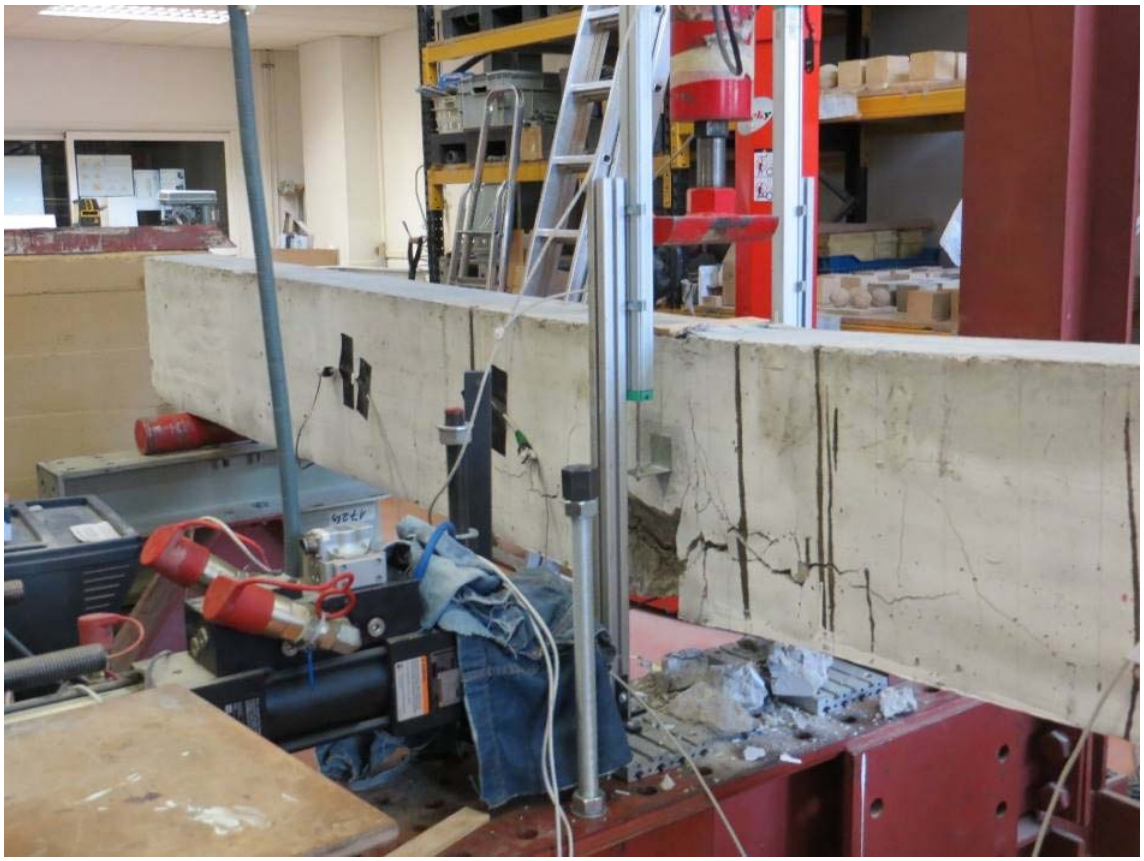

Figure 17. Failure of the FRP-control beam

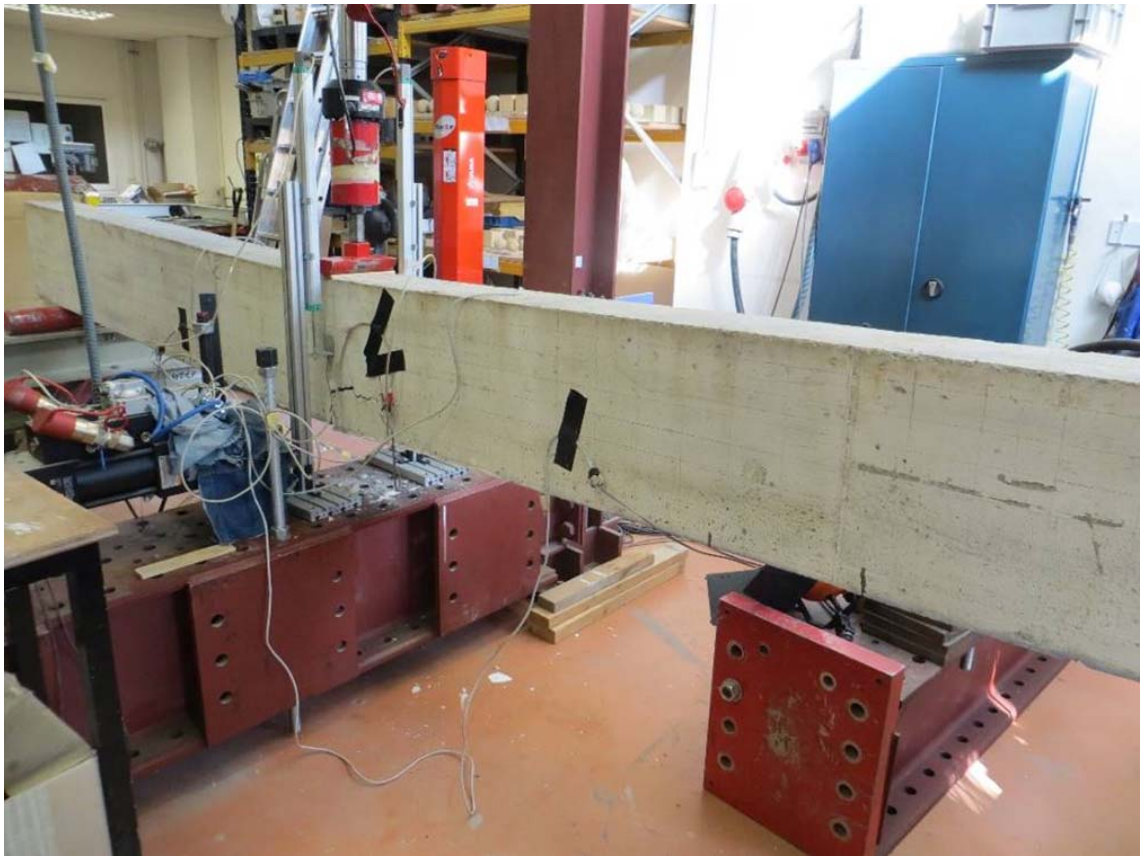

Figure 18. Failure of the FRP post-tensioned beam

Figure 19. Failure of the laminate FRP-control beam

4. Discussion

The post-tensioning process was complex and some construction issues were observed. First, the slits required a perfect geometry; small flaws in the concrete surfaces may make positioning the laminates in the slit difficult. These flaws may also produce frictional problems between the laminate and concrete. Hence, it is important to verify that the slit is clean and perfectly aligned. Second, releasing the actuator and clamping grips produced a small loss of tension in the laminate of up to 3.7% due to handling operations (Table 2).

Table 2. Tension losses in FRP laminates					
Stage	Strain (μm/m)	Stress (N/mm^2)	Force in a single laminate (kN)	Tension losses (%)	Total force (kN) for 2 laminates
Initial load in actuator	5681	124.98	12.50	0.0	25.00
Releasing actuator, clamping ends	5470	120.34	12.03	3.7	24.07
Pouring resin and curing for 48 h	4850	106.70	10.67	14.6	21.34
Ready to test	4822	106.08	10.61	15.1	21.22

Third, because of the viscoelastic nature of the composite laminates, there is also a relevant loss of tension over time. Monitoring the strains in the laminate showed that handling operations (clamping and releasing) produced a small loss of tension, but the more significant losses occurred during the curing of the poured resin. The resin required a period of 48 h to achieve its higher strength, and during this time the laminate was not perfectly bonded and thus relaxed by close to 11%. It is worth mentioning that during the relaxation of the laminates, the resin crystallises, and this hardening of the resin may prevent a larger loss of stress in the laminate. For example, Emara et al. [27] showed that NSM GFRP dramatically modified bond-slip performance during the initial hours, but it stabilised rapidly. In our experiments, the losses did not increase in a relevant manner (only up to 0.5%) for an additional 48 h after resin hardening. Nevertheless, more research is required to effectively balance these contradictory effects and estimate actual losses for BFRP over long time periods. Finally, it is noted that for longer time periods, shrinkage and creep also affect the concrete and thus the problem becomes much more complex, raising questions that are all far beyond the scope of this study.

4.1 First load cycle: Stiffness, cracking moment, strains, and displacements

Table 3 shows that during the first loading cycle, the apparent stiffness of the three beams differed slightly. In Figure 12 the first peak in the plot for each specimen represents the cracking load, which is followed by a descendent slope related to the loss of strength due to cracking. During unloading of the specimen, the plot returns close to the origin. The comparative size of the drop from the peak to the start unloading indicates that the FRP-post-tensioned beam maintains more strength than the other two specimens. The larger this drop, the greater the loss of strength in the specimen. Hence, post-tensioned NSM laminates had a positive effect for preventing loss of strength due to cracking, and the strengthening technique demonstrated its effectiveness.

Table 3. Loads, displacements and stiffness up to the cracking values

		RC-control	FRP-control	FRP-post-tensioned
Pristine (1st load cycle)	Load (kN)	14.5	21.7	25.7
	Displacement (mm)	0.738	0.880	1.222
	Apparent stiffness (N/m)	1.96E+04	2.47E+04	2.10E+04
Post-cracking (2nd load cycle)	Load (kN)	14.5	21.7	25.7
	Displacement (mm)	1.506	1.176	1.476
	Apparent stiffness (N/m)	9.61E+03	1.85E+04	1.74E+04

The cracking moment at the centre of the beam occurs at 14.5 kN·m for the RC-control, 21.7 kN·m for the FRP-control, and 25.7 kN·m for the FRP-post-tensioned specimen. The FRP-post-tensioned beam achieved the highest cracking moment, with an improvement of 77% compared to that of the RC-control. The FRP-control beam also demonstrated an improvement of 50% compared to the RC-control. The laminates had a positive effect against cracking; they stiffened the beam, preventing early cracking (Table 3).

The strain distribution in the mid-span cross-section (Figure 13) showed a linear performance for laminates with similar strain values. However, it should not be forgotten that the post-tensioned laminate had an offset value of 4822 μm/m.

In terms of deformation, the FRP-control beam improved deflection by 19%, whereas the FRP-post-tensioned specimen improved the deflection by a notably 66% compared to the RC-control specimen.

After cracking, all three beams lost stiffness (Table 34). However, the loss was much larger for the RC-control than the FRP beams. While the RC-control lost 51% of its stiffness, the FRP-Control lost 25%, and the FRP-post-tensioned lost only 17%. Therefore, the pre-stressed laminates demonstrate a clear benefit even after cracking.

4.2 Second load cycle: Stiffness, ultimate moment, strains, and displacements

A significant loss in stiffness was observed for the RC-control beam during the second loading cycle. Conversely, FRP-control and FRP-post-tensioned specimens maintained a similar slope (Table 34). Hence, the elastic performance of the NSM laminate played an important role in preventing a large loss of stiffness in the cracked beam. Both FRP-strengthened beams exhibited a clear tri-linear flexural response (Figure 14), and during the non-linear response, the FRP-post-tensioned beam exhibited greater stiffness than the FRP-control beam. Therefore, post-tensioning had a positive effect on the stiffness of the beam compared to the RC-control during both the initial cracked state and the large non-linear state, performing even better than the FRP-control specimen in the latter situation.

The ultimate moment for the RC-control beam is 41.2 kN·m, the FRP-control is 74.1 kN·m, and FRP-post-tensioned is 67.3 kN·m (Table 45). The FRP-control and FRP-post-tensioned specimens both improved the capacity of the beams, by 80% and 63% compared to the RC-control, respectively. NSM technology proved to be very effective for increasing the strength

of specimens. The FRP-control specimen experienced a larger displacement than the FRP-post-tensioned specimen until failure. This is because the tensioned laminates had a previous stress state that limited the total strain of the element. This can be seen in Figure 15, where the laminates show a total strain from the very beginning of the test. The FRP-control and FRP-post-tensioned laminates collapsed and the strain gages failed at 18,000 μm/m.

Figures 16, 17, and 18 show the crack patterns at failure. All of the specimens presented a classical flexural failure. Note that for the FRP post-tensioned beam (Figure 18), the cracks are less open compared to the other two specimens. Therefore, post-tensioning had a positive effect on preventing the opening of cracks. Figure 19 shows the ultimate failure of the FRP laminate and guarantees that the strain on the lower side of beam reached the maximum capacity of the composite material.

Table 4. Load and displacement for the ultimate values

		RC-control	FRP-control	FRP-post-tensioned
Post-cracking (2^{nd} cycle load)	Load (kN)	41.2	74.1	67.3
	Displacement (mm)	67.796	69.512	35.444

The deformations presented in Table 4 indicate that the FRP-control and RC-control specimens had a similar relative deflection, while the FRP-post-tensioned specimen reached a deflection which was 47% less than that of the RC-control. The post-tensioning process induces a counter-deflection, and therefore the final position of the deformed post-tensioned beam is even less with respect to a horizontal reference level, enhancing the strengthening response. Nevertheless, this point was not controlled in this study owing to the manufacturing process.

5. Analytical model and comparisons

General hypothesis for analytical models are:

- Plane sections remain plane.
- Perfect bond exists between materials.
- Shear effects are neglected.
- Tension stiffening is ignored.

5.1 First loading cycle until cracking

During the manufacturing process, self-weight and post-tensioning of the beam did not exceed the cracking moment of the cross-section. Therefore, at the beginning of the tests, all beams were in the elastic uncracked domain.

The proposed model for the flexural response of the RC-control beam and NSM FRP-control and FRP-post-tensioned beams is based on strain compatibility and cross-sectional analysis. The main additional assumptions made include the following:

- All materials exhibit elastic performance.
- The cracking strain in the concrete occurs at the bottom fibres of the cross section.

5.1.1 Cracking moment of unstrengthened beam

According Eurocode 2 [28], the cracking moment in a RC beam, $M_{cr,RC}$, is defined as:

$$M_{cr,RC} = f_{ct,m,fl}\, w_b \tag{2}$$

where $f_{ct,m,fl}$ is the mean flexural tensile strength, and w_b is the elastic section modulus of the gross section; both magnitudes are clearly defined in Eurocode 2 [28]. The characteristic compressive strength can be approached by the experimental value f_c from Table 1 for the material properties. Hence, for our cross section of 200 mm x 400 mm, the cracking moment, $M_{cr,RC}$, is 18.53 kN·m. This theoretical value from Eurocode 2 can be compared to the experimental value obtained during the bending test. It should be noted that total moment over the cross-section is the moment of self-weight (4 kN·m) plus the moment of external load achieved during the first test cycle (see Table 3). Therefore, the experimental value of the cracking moment, $M_{cr,\exp}$, is 18.5 kN·m.

Thus, the experimental result, $M_{cr,\exp}$, perfectly matches the result calculated from the code, $M_{cr,RC}$.

5.1.2 Cracking moments of both strengthened beams

Using a traditional elastic approach for a cross-section composed of different materials with different Young's modulus values (homogenisation theory) and assuming plane strain, it is possible to write equilibrium equations (3) and (4) for the cracking moment, $M_{cr,FRP}$, of both strengthened beams in a general form:

$$\int_A \sigma_c(y)dy + A_{su}\sigma_{yu} - A_{sl}\sigma_{yl} - A_{frp}\sigma_{frp} = N_0 \tag{3}$$

$$\int_A \sigma_c(y)ydy + A_{su}\sigma_{su}(x - d_{su}) + A_{sl}\sigma_{sl}(d_{sl} - x) + A_{frp}\sigma_{frp}(d_{frp} - x) = M_{cr,FRP} - N_0 e \tag{4}$$

where N_0 is the tensile force introduced during the post-tensioning of laminates (when applied), x is the neutral axis, , A is the gross concrete cross section, , A_{su} is the area of the upper rebars, , A_{sl} is the area of the lower rebars, A_{frp} is the area of FRP laminates, , d_{su} is the distance of the upper rebars from the top, , d_{sl} is the distance of the lower rebars from the top, d_{frp} is the distance of the laminate centroid from the top, , σ_c is the concrete stress level, , σ_{su} is the stress level at the upper rebars, , σ_{sl} is the stress level at the lower rebars, , σ_{frp} is the stress level at the laminates, and e is the eccentricity of the cross-section.

The Young's modulus of concrete, E_c, can be approached by E_{cm}, the elastic modulus at 28 d. Then, following Eurocode 2 [28], E_{cm} has a value of 28,576.8 N/mm^2. From the Young's modulus of steel, E_s, and FRP, E_{frp}, it is possible to define the material equivalence coefficients between steel and concrete, n_s, and between FRP and concrete, n_{frp}, as follows:

$$n_s = \frac{E_s}{E_c} = 7.3 \tag{5}$$

$$n_{frp} = \frac{E_{frp}}{E_c} = 0.8 \tag{6}$$

Thus, assuming a plane strain in the cross-section, using simple geometry, it is possible to define the following relationships between the stresses whether the tensile stress in the lower fibre of the concrete is limited:

$$\frac{f_{ct,m,fl}}{h-x} = \frac{\sigma_{su}}{n_s\left(x-d_{su}\right)} = \frac{\sigma_{sl}}{n_s\left(d_{sl}-x\right)} = \frac{\sigma_{frp}}{n_{frp}\left(d_{frp}-x\right)} \tag{7}$$

where h is the total height of the cross-section.

However, using the relationships in equation (7) together with equations (3) and (4) does not produce a proper estimation of the cracking moment, $M_{cr,FRP}$, for the FRP-control beam. The reason probably lies in the elastic tensile strength of concrete based on $f_{ct,m,fl}$. This value is likely modified by the tightening effect of the composite and the resin poured into the slits, and thus it might have a higher value. Hence, increasing $f_{ct,m,fl}$ by a factor of 1.2, and using the relationships in equation (7) with equilibrium equations (3) and (4) results in a $M_{cr,FRP}$ of 24 kN·m. This is in good agreement with the experimental value of FRP-control, $M_{cr,FRP,\exp}$, of 24.7 kN·m (from Table 3 and including the self-weight).

For the FRP-post-tensioned beam, using the relationships in equation (7) together with equations (3) and (4) and values for the force from Table 2 for N_0 does not produce a proper estimation of the cracking moment. However, by increasing $f_{ct,m,fl}$ by a factor of 1.3, a good agreement with the experimental value can be achieved; $M_{cr,FRP}$ is 30 kN·m, and the experimental value, $M_{cr,FRP,\exp}$, is 29.7 kN·m (from Table 3 and including the self-weight). This factor (1.3) is higher than for the FRP-control beam (1.2) because the post-tensioning load may increase the tightening effect over the concrete.

5.2 Second loading cycle until failure

The ultimate values are far from the elastic domain, and generalised cracking occurred in all beams. In the experiments, failure occurred in the RC-control beam due to the steel bottom rebars failing, while in the NSM beams, failure occurred when the composite fibres reached an ultimate tensile strain. Moreover, from the measured strain levels, the bottom steel rebars are inside the plastic branch of the material law.

5.2.1 Ultimate moment of the unstrengthened beam

In this case, the tensile strain of the lower steel rebars is 0.01 (or larger). Using Eurocode 2 [28],] it is possible to write the equilibrium equation to determine the position of the neutral axis, x, and the ultimate moment, $M_{u,RC}$, as follows:

$$\int_A \sigma_c(y)dy - A_{sl} f_{yl} = b0.8xf_c - A_{sl} f_y = 0 \quad (8)$$

$$\int_A \sigma_c(y)ydy + A_{sl}\sigma_{sl}(d_{sl} - x) = M_{u,RC} \quad (9)$$

Using values for the materials from Table 1, the ultimate moment for the RC beam, $M_{u,RC}$, is 41.1 kN·m. This value must be compared with the experimental moment calculated using the moment of the experimental load (Table 4) plus the self-weight moment. This gives an experimental value, $M_{u,\exp}$, of 45.2 kN·m, which is larger than the theoretical value of 41.1 kN·m (an error of 9%). This discrepancy is not outside the acceptable range in experimental mechanics. However, the actual value for the ultimate strength of steel is probably higher than 500 MPa, as the authors have observed in other similar experiments, and this increase could explain the discrepancy.

5.2.2 Ultimate moments of both strengthened beams

In both cases, the tensile strain of the composite laminate reaches the value obtained with equation (1). Note that this strain is the same for the lower steel bars. This means that the steel rebars in the bottom part of the beam are close to their ultimate failure with a clear excess from the limitation of Eurocode 2 for the design ($10\ ‰$). Therefore, the bottom rebars are under a known stress, f_y.

Thus, it is possible to write the equilibrium equations in a general manner as follows:

$$\int_A \sigma_c(y)dy - A_{sl}\sigma_{yl} - A_{frp}\sigma_{frp} = f_c b0.8x - A_{sl} f_y - A_{frp} f_{frp} = N_0 \quad (19)$$

$$\int_A \sigma_c(y)ydy + A_{su}\sigma_{su}(x - d_{su}) + A_{sl}\sigma_{sl}(d_{sl} - x) + A_{frp}\sigma_{frp}(d_{frp} - x) = M_{u,FRP} - N_0 e \quad (20)$$

Using the values for the materials listed in Table 1, the ultimate moment of the FRP-control beam, $M_{u,FRP}$, is 71.86 kN·m. This value must be compared with the experimental value. The moment of the experimental load for the FRP-control beam (Table 4) plus the self-weight moment gives an experimental value, $M_{u,FRP,\exp}$, of 78.1 kN·m, which is larger than the

theoretical value of 71.8 kN·m (8% error). This discrepancy could be attributed to the same factors as with the RC beam.

For the FRP-post-tensioned beam, using the values for the materials listed in Table 1 and the N_0 from Table 2, the ultimate moment, $M_{u,FRP}$, is 64.50 kN·m. The moment of the experimental load (Table 4) plus the self-weight moment result in a value of 71.3 kN·m for the ultimate experimental moment, $M_{u,FRP,\exp}$. Again, the experimental value is larger than the theoretical value of 64.50 kN·m (9% error). This discrepancy could be in the same sense as that for the RC and FRP-control beams.

6. Conclusions

This work experimentally investigates NSM post-tensioned strengthening with BFRP laminates for concrete beams. The study compares the experimental performance of a pristine concrete beam (RC-control), a beam strengthened with NSM BFRP laminates without post-tensioning (FRP-control), and a beam with NSM post-tensioned BFRP laminates (FRP-post-tensioned). The level of post-tensioning compensates for the effect of self-weight. All beams were tested in a three point bending test with displacement control.

- Practitioners must take care during slit manufacturing because small defects may affect the alignment of laminates and prevent effective post-tensioning.
- Post-tensioned BFRP laminates suffer tension losses of close to 15%, which appear to stabilise after 96 h. The viscoelastic nature of the laminate matrix and the resin poured in the slit explains this performance. Nevertheless, additional research is required to effectively balance these losses and the level of prestressing.
- An analytical approach using the plane cross-section and equilibrium can provide reasonable values. The cracking moment is improved with the post-tensioning technique, rising by 77% compared to the RC-control and 50% compared to the FRP-control. These experimental values agree with the analytical formulation if the elastic tensile strength of concrete is increased by a factor of 1.2 in the non-post-tensioned FRP beam and a factor of 1.3 in the post-tensioned beam. This is justified by the local tightening effect on the concrete of the NSM technique.
- The ultimate load also improves with post-tensioning by up to 63% compared to the RC-control. However, the FRP-control was more competitive in this respect, achieving an improvement of 80%, because the pre-stressed state of the FRP-post-tensioned beam induced faster failure. The analytical values need to increase the ultimate strength of steel by around 9%, as the authors found in other experimental campaigns, to match the experimental results.
- Deflection control is the aspect where the post-tensioned beam was most competitive, for both the cracking and ultimate states. The level of relative deflection was reduced dramatically. Until cracking, deflection with the FRP-post-tensioned beam was 66% more effective than with the RC-control, while the FRP-control only achieved an improvement of 19%. For the ultimate values, the RC-control and FRP-control beams achieved similar deflections, while the FRP-post-tensioned beam reduced the deformation by 47%. These values could even be more favourable for the FRP post-

tensioned beam if the absolute values of displacement and the counter-deflection during laminate prestressing were considered.

- After cracking, the effective stiffness decreased by up to 52% in the RC-control, 26% in the FRP-control, and only 18% in the FRP-post-tensioned specimen. This shows that post-tensioning is an effective technique which can prevent loss of stiffness even after cracking.

7. References

[1] FIB CEB-FIP. Bulletin 14. “Externally bonded FRP reinforcement for RC structures”. 2001.

[2] Nordin, Hakan;H, Taljsten, Bjorn. “Concrete beams strengthened with prestressed near surface mounted CFRP”. Journal of Composites for Construction, ISSN 1090-0268, Volume 10, Issue1, Pages 60-8, (2006).

[3] Badawi, Moataz; Soudki, Khaled. “Flexural strengthening of RC beams with prestressed NSM CFRP rods-experimental and analytical investigation”. Construction and Building Materials, ISSN: 0950-0618, Volume 23, Issue 10, Pages 3292-3300, (2009).

[4] Peng, Hui; Zhang, Jianren; Cai, C.S. ; Liu, Yang. “An experimental study on reinforced concrete beams strengthened with prestressed near surface mounted CFRP strips”, Engineering Structures, ISSN 0141-0296, Volume 79, Pages 222-233, (2014).

[5] Kara, Ilker Fatih; Ashour, Ashraf F. ; Köroğlu, Mehmet Alpaslan. “Flexural performance of reinforced concrete beams strengthened with prestressed near-surface-mounted FRP reinforcements”, Composites Part B: Engineering, ISSN 1359-8368, Volume 91, Pages 371-383, (2016).

[6] Hong, Sungnam ; Park, Sun-Kyu. “Effect of prestress and transverse grooves on reinforced concrete beams prestressed with near-surface-mounted carbon fiber-reinforced polymer plates”. Composites Part B: Engineering, ISSN 1359-8368, Volume 91, Pages 640-650, (2016).

[7] Hosseini, M.R. Mostakhdemin ; Dias, S.J.E. ; Barros, J.A.O. “Effectiveness of prestressed NSM CFRP laminates for the flexural strengthening of RC slabs”, Composite Structures, ISSN 0263-8223, Volume 111, Pages 249-258, (2014).

[8] Hosseini, M. R. Mostakhdemin; Dias, S. J. E. and Barros, J. A. O.. “Flexural strengthening of reinforced low strength concrete slabs using prestressed NSM CFRP laminates”. Composites Part B: Engineering, ISSN 1359-8368, Volume 90, Pages 14–29, (2016).

[9] Kotynia, Renata; Lasek, Krzysztof and Staskiewicz, Michal. “Flexural behavior of preloaded (RC) slabs strengthened with prestressed CFRP laminates”. Journal of Composites for Construction, ISSN 1090-0268, Volume 18, Issue 3, Pages 1-11, (2014).

[10] Si-Larbi, Amir; Agbossou, Amen; Ferrier, Emmanuel; Michel, Laurent. “Strengthening RC beams with composite fiber cement plate reinforced by prestressed FRP rods: Experimental and numerical analysis”, Composite Structures, ISSN 0263-8223, Volume 94, Issue 3, Pages 830-838, (2012).

[11] Rezazadeh, Mohammadali; Barros, Joaquim; Costa, Inês. “Analytical approach for the flexural analysis of RC beams strengthened with prestressed CFRP”, Composites Part B: Engineering, ISSN 1359-8368, Volume 73, Pages 16-34, (2015).

[12] El-Hacha, Raatfat and Gaafar, Mohamed. “Flexural strengthening of reinforced concrete beams using prestressed, near surface mounted CFRP bars. PCI Journal. ISSN 08879672, Volume 56, 134–151, (2011).

[13] Kotynia , Renata and Przygocka, Marta. “Preloading Effect on Strengthening Efficiency of RC Beams Strengthened with Non-and Pretensioned NSM Strips”. Polymers ISSN 2073-4360, Volume 10, Issue 2, 145, Pages 1-14, (2018).

[14] Aslam, Muhammad; Shafigh, Payam; Jumaat, Mohd Zamin; Shah, S N R. “Strengthening of RC beams using prestressed fiber reinforced polymers – A review”. Construction and Building Materials, ISSN: 0950-0618, Volume 82, Pages 235–256, (2015).

[15] Michels, Julien; Barros, Joaquim; Costa, Inês; Sena-Cruz, José; Czaderski, Christoph; Giacomin, Giorgio; Kotynia, Renata; Lees, Janet; Pellegrino, Carlo and Zile, Edmunds. “Chapter 7 Prestressed FRP Systems”. *Design Procedures for the Use of Composites in Strengthening of Reinforced Concrete Structures*. C. Pellegrino and J. Sena-Cruz (eds.), RILEM State-of-the-Art Reports 19, DOI 10.1007/978-94-017-7336-2_7. (2016).

[16] Zhang, S.S.; Yu, T. and Chen, G.M. “Reinforced concrete beams strengthened in flexure with near-surface mounted (NSM) CFRP strips: Current status and research needs”. Composites Part B: Engineering, ISSN 1359-8368, Volume 131, Pages 30–42, (2017).

[17] Pellegrino, Carlo and Modena, Claudio. “Flexural strengthening of real-scale RC and PRC beams with end-anchored pretensioned FRP laminates”. ACI Structural Journal, ISSN 08893241, Volume 106, Num 3, Pages 319-328, (2009).

[18] Michels, Julien; Martinelli, Enzo; Czaderski, Christoph and Motavalli, Masoud. “Prestressed CFRP strips with gradient anchorage for structural concrete retrofitting: experiments and numerical modelling”. Polymers ISSN 2073-4360, Volume 6, Issue 1, Pages 114-131, (2014).

[19] Triantafyllou, Garyfalia G.; Rousakis, Theodoros C. and Karabinis, Athanasios I. “Analytical assessment of the bearing capacity of RC beams with corroded steel bars beyond concrete cover cracking.”. Composites Part B: Engineering, ISSN 1359-8368, Volume 119, Pages 1325-140, (2017).

[20] Triantafyllou, Garyfalia G.; Rousakis, Theodoros C. and Karabinis, Athanasios I. “Corroded RC beams patch repaired and strengthened in flexure with fiber-reinforced polymer laminates”. Composites Part B: Engineering, ISSN 1359-8368, Volume 112, Pages 125-136, (2017).

[21] Triantafyllou, Garyfalia G.; Rousakis, Theodoros C. and Karabinis, Athanasios I. “Effect of patch repair and strengthening with EBR and NSM CFRP laminates for RC beams with low, medium and heavy corrosion”. Composites Part B: Engineering, ISSN 1359-8368, Volume 133, Pages 101-111, (2018).

[22] Charalambidi, Barbara G.; Rousakis, Theodoros C. and Karabinis, Athanasios I. “Fatigue behavior of large-scale reinforced concrete beams strengthened in flexure with fiber-reinforced polymer laminates”. Journal of Composites for Construction, ISSN 1090-0268, Volume 20, Issue 5, (2016).

[23] Charalambidi, Barbara G.; Rousakis, Theodoros C. and Karabinis, Athanasios I. “Analysis of the fatigue behavior of reinforced concrete beams strengthened in flexure with fiber

reinforced polymer laminates", Composites Part B: Engineering, ISSN 1359-8368, Volume 96, Pages 69-78, (2016).

[24] EN 12390 "Testing hardened concrete - Part 3: Compressive strength of test specimens".

[25] EN ISO 527-4 "Plastics. Determination of tensile properties - Part 4: Test conditions for isotropic and orthotropic fibre-reinforced plastic composites".

[26] Lord, Jerry David and Morell, Roger M. "Elastic modulus measurement—obtaining reliable data from the tensile test". Metrologia, ISSN 0026-1394, Volume 47, N.2, Pages S41. (2010).

[27] Emara, Mohamed; Torres, Lluís; Baena, Marta; Barris, Cristina; Cahís, Xavier. "Bond response of NSM CFRP strips in concrete under sustained loading and different temperature and humidity conditions". Composite Structures, ISSN 0263-8223, Volume 192, Pages 1-7, (2018).

[28] EN1992-1-1 "Eurocode 2: Design of concrete structures".